

Transverse Spin Structure of the Nucleon through Target Single Spin Asymmetry in Semi-Inclusive Deep-Inelastic ($e, e'\pi^\pm$) Reaction at Jefferson Lab

H. Gao¹, L. Gamberg², J.-P. Chen³, X. Qian⁴, Y. Qiang³, M. Huang¹, A. Afanasev⁵,
M. Anselmino⁶, H. Avakian³, G. Cates⁷, E. Chudakov³, E. Cisbani⁸, C. de Jager³,
F. Garibaldi⁸, B.T. Hu⁹, X. Jiang¹⁰, K. S. Kumar¹¹, X.M. Li¹², H.J. Lu¹³, Z.-E. Meziani¹⁴,
B.-Q. Ma¹⁵, Y.J. Mao¹⁵, J.-C. Peng¹⁶, A. Prokudin³, M. Schlegel¹⁷,
P. Souder¹⁸, Z.G. Xiao¹⁹, Y. Ye²⁰, L. Zhu⁵

¹*Duke University, Durham, NC 27708, USA*

²*Penn State University-Berks, Reading, PA 19610, USA*

³*Jefferson Lab, Newport News, VA 23606, USA*

⁴*Kellogg Radiation Laboratory, California Institute of Technology, Pasadena, CA 91125, U.S.A.*

⁵*Hampton University, Hampton, VA 23668, USA*

⁶*Universita di Torino and INFN, Sezione di Torino, I-10125, Torino, Italy*

⁷*University of Virginia, Charlottesville, VA 22901, USA*

⁸*INFN, Sezione di Roma III, 00146 Roma, Italy*

⁹*Lanzhou University, Lanzhou, P.R. China*

¹⁰*Los Alamos National Laboratory, Los Alamos, NM, USA*

¹¹*University of Massachusetts, Amherst, MA 01003, USA*

¹²*China Institute of Atomic Energy, Beijing, P.R. China*

¹³*Huangshan University, Huangshan, P.R. China*

¹⁴*Temple University, Philadelphia, PA 19122, USA*

¹⁵*School of Physics, Peking University, Beijing, P.R. China*

¹⁶*University of Illinois at Urbana-Champaign, Urbana, IL 61801, USA*

¹⁷*Institute for Theoretical Physics, Universität Tübingen, D-72076 Tübingen, Germany*

¹⁸*Syracuse University, Syracuse, NY 13244, USA*

¹⁹*Tsinghua University, Beijing, P.R. China*

²⁰*University of Science and Technology, Hefei, P.R. China*

Abstract

Jefferson Lab (JLab) 12 GeV energy upgrade provides a golden opportunity to perform precision studies of the transverse spin and transverse-momentum-dependent structure in the valence quark region for both the proton and the neutron. In this paper, we focus our discussion on a recently approved experiment on the neutron as an example of the precision studies planned at JLab. The new experiment will perform precision measurements of target Single Spin Asymmetries (SSA) from semi-inclusive electro-production of charged pions from a 40-cm long transversely polarized ^3He target in Deep-Inelastic-Scattering kinematics using 11 and 8.8 GeV electron beams. This new coincidence experiment in Hall A will employ a newly proposed solenoid spectrometer (SoLID). The large acceptance spectrometer and the high polarized luminosity will provide precise 4-D (x , z , P_T and Q^2) data on the Collins, Sivers, and pretzelosity asymmetries for the neutron through the azimuthal angular dependence. The full 2π azimuthal angular coverage in the lab is essential in controlling the systematic uncertainties. The results from this experiment, when combined with the proton Collins asymmetry measurement and the Collins fragmentation function determined from the e^+e^- collision data, will allow for a quark flavor separation in order to achieve a determination of the tensor charge of the d quark to a 10% accuracy. The extracted Sivers and pretzelosity asymmetries will provide important information to understand the correlations between the quark orbital angular momentum and the nucleon spin and between the quark spin and nucleon spin.

1 Introduction

Deep inelastic lepton-nucleon scattering (DIS) experiments have played a fundamental role in describing the partonic momentum structure of hadrons. The unpolarized parton distribution functions (PDF) have been extracted with excellent precision over a large range of x and Q^2 from DIS, Drell-Yan and other processes after several decades of experimental and theoretical efforts. The comparison of the structure functions in the large Q^2 range with QCD evolution equations has provided one of the best tests of QCD.

When the target and/or beam are polarized the essential properties of spin-angular momentum structure of hadrons is probed. Three decades of intensive experimental and theoretical investigation have resulted in a great deal of knowledge on the partonic origin of the nucleon spin structure. Motivated by the “spin crisis” from the European Muon Collaboration experiment in the 1980s [1], the longitudinal polarized parton distribution functions have been determined with significantly improved precision over a large region of x and Q^2 from polarized deep-inelastic (DIS) experiments carried out at CERN, SLAC, DESY in the last two decades, and more recently at JLab and at RHIC from polarized proton-proton scattering (see [2, 3] for reviews and compilation of references). In particular, considerable knowledge has been gained from inclusive DIS experiments on the longitudinal structure – the x -dependence and the helicity distributions – in terms of the unpolarized (denoted $q^a(x)$ or $f_1^a(x)$) and helicity (denoted $\Delta q^a(x)$ or $g_1^a(x)$) parton distribution functions for the various flavors (indicated by a).

In more recent experimental and theoretical studies, it has become evident that precise knowledge of the transverse structure of partons is essential to unfold the full momentum and spin structure of the nucleon. This concerns in particular the investigations of the chiral-odd transversely polarized quark distribution function or transversity [4] (denoted as $\delta q(x)$, $h_1(x)$ or also $\Delta_T q(x)$) which is probed in transverse spin polarization experiments. Like the axial charge $\Delta q^a = \int_0^1 dx (g_1^a(x) + g_{\bar{1}}^a(x))$, the tensor charge $\delta q^a = \int_0^1 dx (h_1^a(x) - h_{\bar{1}}^a(x))$ is a basic property of the nucleon. The essential role of the transversity distribution function emerges from a systematic extension of the QCD parton model to include transverse momentum and spin degrees of freedom. In this context, semi-inclusive deep-inelastic lepton nucleon scattering (SIDIS) has emerged as an essential tool to probe both the longitudinal and transverse momentum and spin structure of the nucleon. The azimuthal dependence in the scattering of leptons off transversely polarized nucleons is explored through the analysis of transverse single spin asymmetries (TSSAs). Recent work [5, 6, 7] predicts that these observables are factorized convolutions of leading-twist transverse momentum dependent parton distributions (TMDs) and fragmentation functions (FFs). These functions provide *essential non-perturbative* information on the partonic sub-structure of the nucleon; they offer a rich understanding of the motion of partons inside the nucleon, of the quark orbital properties, and of spin-orbit correlations. They also provide essential information on multi-parton correlations at leading-twist, allowing us to explore and uncover the dynamics of the quark-gluon structure of the nucleon.

At leading twist if we integrate over the transverse momenta of quarks, the three quark distribution functions remain: the unpolarized parton distribution f_1 , the longitudinal polarized parton distribution g_1 , and the quark transversity distribution h_1 . Besides f_1 , g_1 and h_1 , there are five more transverse momentum dependent distribution functions [5, 6]. Since these TMDs provide the description of the parton distributions beyond the collinear approximation, they depend not only on the longitudinal momentum fraction x , but also on the transverse momentum, k_T . An intuitive interpretation of the k_T dependent transversity distribution, h_1 , is that it gives

the probability of finding a transversely polarized parton inside a transversely polarized nucleon with certain longitudinal momentum fraction x and transverse momentum k_T .

The JLab 12 GeV upgrade provides a unique opportunity to extend our understanding of nucleon spin and momentum structure by carrying out multi-dimensional precision studies of longitudinal and transverse spin and momentum degrees of freedom from SIDIS experiments with high luminosity in combination with large acceptance detectors. Such a program will provide the much needed kinematic reach to unfold the generalized momentum and flavor structure of the nucleon. In the next section, we summarize the essential role that transverse polarization studies play in unfolding this structure in SIDIS.

2 Transverse Structure and Semi-Inclusive DIS

The transverse spin and momentum structure of the nucleon was discussed in the context of polarized proton-proton scattering experiments by Hidaka, Monsay and Sivers [8] in 1978 and in Drell-Yan Scattering by Ralston and Soper [9] in 1979. Early theoretical analysis of the transversity distribution of the nucleon was studied by Artru [4] and a more thorough treatment was given by Jaffe and Ji in early 1990s [10] where they introduced the tensor charge in the context of the QCD parton model.

The transversity function is a chirally odd quark distribution function, and the least known among the three leading twist parton distribution functions. It describes the net quark transverse polarization in a transversely polarized nucleon [10]. In the non-relativistic limit, the transversity distribution function $h_1(x, Q^2)$ is the same as the longitudinal quark polarization distribution function, $g_1(x, Q^2)$. Therefore, the transversity distribution function probes the relativistic nature of the quarks inside the nucleon.

There are several interesting properties of the quark transversity distribution. First it does not mix with gluons; that is, it evolves as a non-singlet distribution [11] and doesn't mix with gluons under evolution and thus has valence-like behavior [12]. Secondly in the context of the parton model it satisfies the Soffer bound [13], which is an inequality among the three leading twist distributions, $|h_1^q| \leq \frac{1}{2}(f_1^q + g_1^q)$, based on unitarity and parity conservation. QCD evolution of transversity was studied in Ref. [14], where it was shown that Soffer's inequality holds up to next to leading order (NLO) QCD corrections. In the past [15] and more recently [16], studies have been performed that consider the violation of this bound. Therefore, it is interesting to experimentally test the Soffer's inequality as a function of Q^2 . Lastly, the lowest moment of h_1^q is the tensor charge, which has been calculated from lattice QCD [17] and various models [18, 19, 20, 21, 22, 23]. Due to the valence-like nature of the transversity distribution, measuring transversity in the high- x region (JLab kinematics) is crucial to determine tensor charge of quarks. The experimental determination of the transversity function is challenging - it is not accessible in polarized inclusive DIS measurements when neglecting quark masses - h_1 decouples at leading twist in an expansion of inverse powers of the hard scale in inclusive deep-inelastic scattering due to the helicity conserving property of the QCD interactions. However, paired with another hadron in the initial state *e.g.* double polarized Drell-Yan processes with (two transversity distributions) [9], or in the final state, *e.g.* semi-inclusive deep-inelastic [24] scattering (transversity and Collins fragmentation function), leading twist h_1 can be accessed without suppression by a hard scale.

The most feasible way to access the transversity distribution function is via an azimuthal

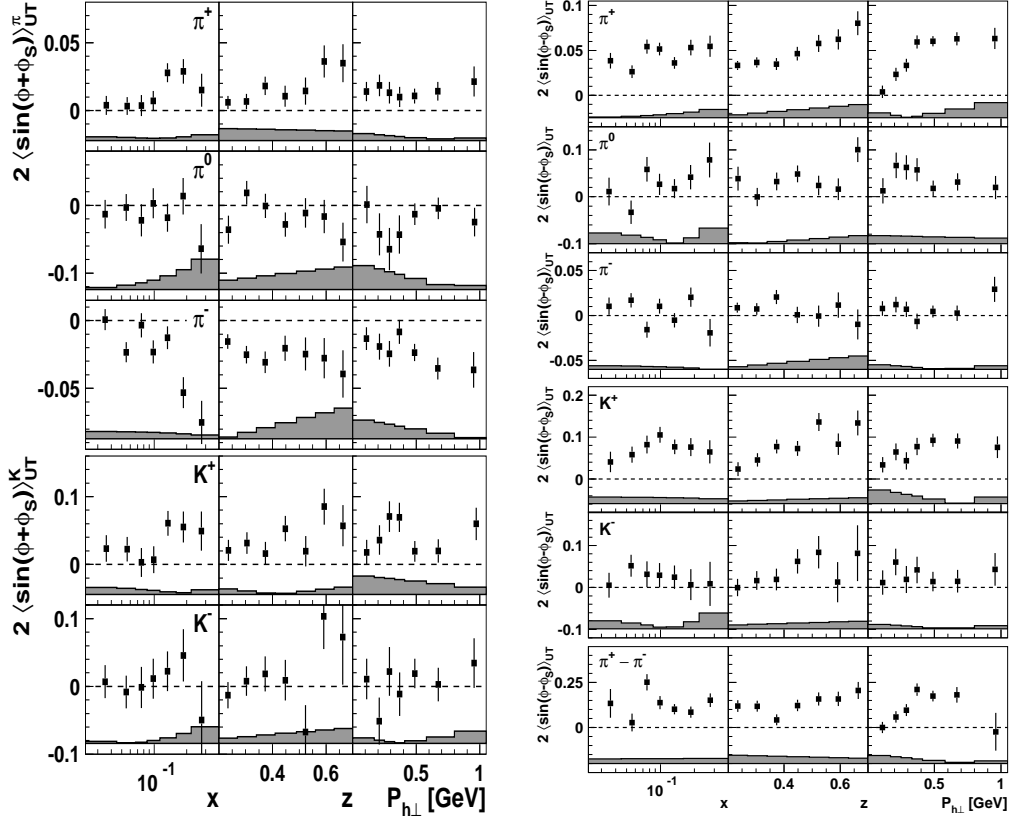


Figure 1: Left Panel: From [25], Collins amplitudes for pions and charged kaons as a function of x , z , or p_{\perp} . The systematic uncertainty is given as a band at the bottom of each panel. In addition there is a 7.3% scale uncertainty from the accuracy in the measurement of the target polarization. Right panel: From [26], Siverson amplitudes for pions, charged kaons, and the pion-difference asymmetry (as denoted in the panels) as functions of x , z , or p_{\perp} . The rest of the caption is the same as in the left panel.

single spin asymmetry, in semi-inclusive deep-inelastic lepto-production of mesons on a transversely polarized nucleon target, $eN^{\uparrow} \rightarrow e\pi X$. In this case the other chiral-odd partner is the Collins fragmentation function, H_1^{\perp} [24]. Schematically with factorization, this transverse single spin asymmetry (TSSA) contains h_1 and H_1^{\perp} , $A_{UT} \sim h_1 \otimes H_1^{\perp}$ ($U \equiv$ unpolarized lepton beam, $T \equiv$ transversely polarized target) [6]. The Collins function is one of a class of so-called *naive time reversal odd* (T-odd) transverse momentum dependent fragmentation functions - the existence of which has far reaching consequences for factorization theorems and the application of color gauge invariance to nucleon structure.

The first evidence of non-trivial transverse spin effects in SIDIS has been observed in the transverse single spin asymmetries measured by the HERMES [25, 26, 28] and the COMPASS [27] experiments where an unpolarized lepton beam is scattered off a transversely polarized proton target, $lp^{\uparrow} \rightarrow l'hX$ (see Figures 1 and 2). Besides the non-zero Collins asymmetry, which contains h_1 and H_1^{\perp} discussed previously, another non-zero asymmetry (Sivers asymmetry), was also observed. The Sivers asymmetry is associated with a naive T-odd transverse momentum

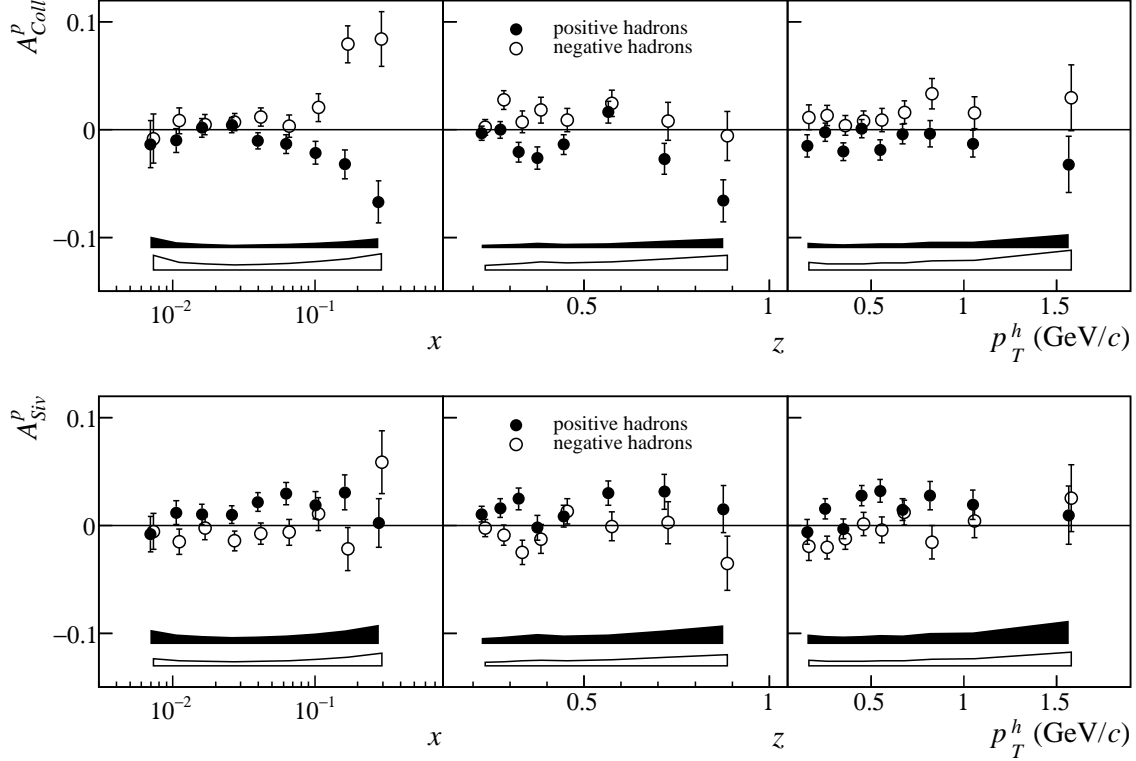


Figure 2: Upper Panel: From [27], the Collins asymmetry as a function of x , z , and p_T^h , for positive (closed points) and negative (open points) hadrons. The bars show the statistical errors. The point to point systematic uncertainties have been estimated to be $0.5 \sigma_{stat}$ for positive and $0.6 \sigma_{stat}$ for negative hadrons and are given by the bands. Lower Panel: From [27], the Sivers asymmetry as a function of x , z , and p_T^h , for positive (closed points) and negative (open points) hadrons. The bars show the statistical errors. The point to point systematic uncertainties are given by the bands. For positive hadrons only, an absolute scale uncertainty of ± 0.01 has also to be taken into account.

dependent (TMD) parton distribution function [29]. By contrast to inclusive deep-inelastic lepton-nucleon scattering where transverse momentum is integrated out, these processes are sensitive to the transverse-momentum scale, P_T , which is on the order of the intrinsic quark momentum, k_T ; that is $P_T \sim k_T$. This is evident by considering the generic structure of the TSSA for a transversely polarized nucleon target which is characterized by interference between helicity flip and helicity non-flip amplitudes $A_{UT} \sim \text{Im}(f^{*+} f^-)$. In the collinear limit of QCD, partonic processes conserve helicity and Born amplitudes are real [30]. For this structure to be non-zero at leading twist we must go beyond the collinear limit where such a reaction mechanism requires a recoil scale sensitive to the intrinsic quark transverse momentum. This is roughly set by the confinement scale $k_T \sim \Lambda_{QCD}$ [31]. Because strongly interacting processes conserve parity transverse spin asymmetries are described by T-odd correlations between transverse spin \mathbf{S}_T , longitudinal momentum \mathbf{P} and intrinsic quark momentum \mathbf{k}_T [29, 24], which are depicted by the generic vector product $i\mathbf{S}_T \cdot (\mathbf{P} \times \mathbf{k}_\perp)$. These correlations imply a leading twist reaction

mechanism which is associated with a naive T-odd transverse momentum dependent (TMD) parton distribution [29] and fragmentation [24] function (PDF & FF).

A crucial theoretical breakthrough [32, 33, 34] was that the reaction mechanism is due to non-trivial phases arising from the color gauge invariant property of QCD. This leads to the picture that TSSAs arise from initial and final state interactions [35, 36, 37] (ISI/FSI) of the active quark with the soft distribution or fragmentation remnant in SIDIS, which manifests itself as a gauge link that links the bilocal quark configuration. This gauge link gives rise to the final state gluonic interactions between the active quark and target remnant. Thus, T-odd TMDs are of crucial importance because they possess transverse spin polarization structure as well as the necessary phases to account for TSSAs at leading twist. Further work on factorization theorems for SIDIS indicate that there are two leading twist T-odd TMDs; the Sivers function, denoted as f_{1T}^\perp describing the probability density of finding unpolarized partons inside a transversely polarized proton, is one of these functions, while the Boer-Mulders function h_1^\perp describes the probability density of finding a transversely polarized quark inside a unpolarized nucleon by virtue of the color gauge invariant symmetry of QCD. All these aforementioned ingredients (TMD, FF, gauge link) enter the factorized [7] hadronic tensor for semi-inclusive deep-inelastic scattering.

Exploring the transverse spin structure of the TMD PDFs reveals evidence of a rich spin-orbit structure of the nucleon. When the transverse spin and momentum correlations are associated with the nucleon, where the quark remains *unpolarized*, the Sivers function [29] describes the helicity flip of the nucleon target in a helicity basis. Since the quark is unpolarized in the Sivers function, the orbital angular momentum of the quarks must come into play to conserve overall angular momentum in the process [38, 39]. This result has a far-reaching impact on the QCD theory of generalized angular momentum [40]. Indeed a partonic description of the Sivers and Boer-Mulders functions requires wave function components with nonzero orbital angular momentum and thus provides information about the correlation between the quark orbital angular momentum (OAM) and the nucleon/quark spin, respectively [35, 40].

Unlike the Sivers and Boer-Mulders functions, which provide a clean probe of the QCD FSI, the functions g_{1T} and h_{1L}^\perp are (naive) T-even, and thus do not require FSI to be nonzero. Nevertheless, they also require interference between wave function components that differ by one unit of OAM and thus require OAM to be nonzero. Finally, the pretzelosity h_{1T}^\perp requires interference between wave function components that differ by two units of OAM (e.g. p-p or s-d interference). Combining the wealth of information from all these functions could be invaluable for disentangling the spin orbit correlations in the nucleon wave function, thus providing important information about the quark orbital angular momentum.

Complementary to Generalized Parton distributions (or Impact Parameter Dependent distributions), which describe the probability of finding a parton with certain longitudinal momentum fraction and at certain transverse position b (1-D momentum space and 2-D coordinate space), TMDs give a description of the nucleon structure in 3-D momentum space. Furthermore, by including the transverse momentum of the quark, the TMDs reveal important information about the nucleon/parton spin-orbital angular momentum correlations.

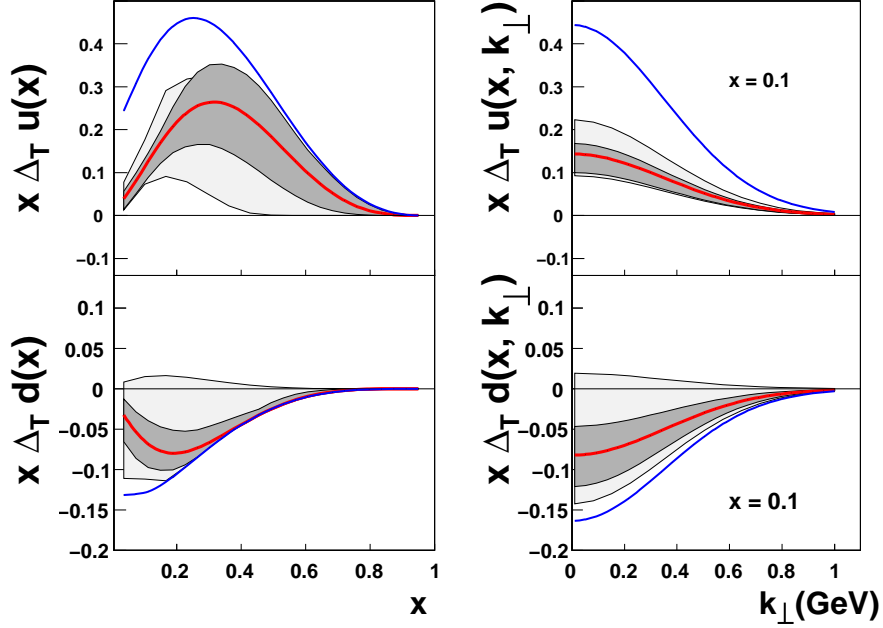


Figure 3: From [41], the transversity distribution functions for u and d flavors as determined by a global fit analysis, at $Q^2 = 2.4 \text{ GeV}^2$ [41]. The Soffer bound [13] (highest or lowest lines) and the (wider) uncertainty bands of a previous extraction [42] are displayed.

3 The Phenomenology TSSAs and TMDs

All eight leading twist TMDs can be accessed in SIDIS. In this paper, we focus on three of them: transversity, Sivers, and pretzelosity, which can be accessed through a transversely polarized target. There are three mechanisms which can lead to the single (transversely polarized target) spin azimuthal asymmetries, which are the Collins asymmetry, the Sivers asymmetry, and the pretzelosity asymmetry. As mentioned in Section 2 the quark transversity function in combination with the chiral-odd Collins fragmentation function [24] gives rise to an azimuthal (Collins) asymmetry in $\sin(\phi_h + \phi_S)$, where azimuthal angles of both the hadron (pion) (ϕ_h) and the target spin (ϕ_S) are with respect to the virtual photon axis and relative to the lepton scattering plane. The Sivers asymmetry [45, 29, 46] refers to the azimuthal asymmetry in $\sin(\phi_h - \phi_S)$ due to the correlation between the transverse target polarization of the nucleon and the transverse momentum of the quarks, which involves the orbital angular momentum of the unpolarized quarks [35, 38]. The pretzelosity asymmetry is similar to Collins asymmetry except it is due to quarks polarized perpendicularly to the nucleon spin direction in the transverse plane in a transversely polarized nucleon. It has an azimuthal angular dependence of $\sin(3\phi_h - \phi_S)$. One can disentangle these angular distributions by taking the azimuthal moments of the asymmetries as has been done by the HERMES Collaboration [28] and the COMPASS Collaboration [47].

In recent years a great deal of understanding of transverse spin effects, final state interactions, and the spin orbit structure of partonic-hadronic interactions has been gained from model

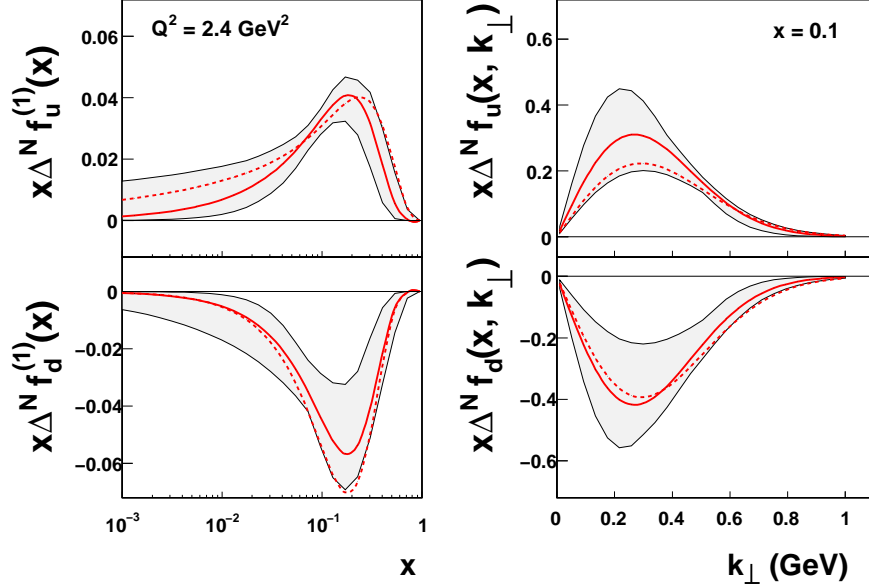


Figure 4: From [43], the Siverts distribution functions for u and d flavors, at the scale $Q^2 = 2.4$ $(\text{GeV}/c)^2$, as determined by an updated model-dependent fit (solid lines) are compared with those of an earlier fit [44] of SIDIS data (dashed lines), where π^0 and kaon productions were not considered and only valence quark contributions were taken into account. This plot shows that the Siverts functions previously found are consistent, within the statistical uncertainty bands, with the Siverts functions obtained in [43].

calculations of the TMDs and fragmentation functions. In particular the final state interactions in TSSAs through the Siverts function has been studied in spectator models and the light-cone wave function approach [35, 36, 37, 48, 49, 50, 51, 52] as well as the bag model [53]. The Collins function has been calculated in [54, 55] while studies of the universality of T-odd fragmentation functions have been carried out in [56, 57, 58]. The Boer-Mulders function has been calculated in [59, 37, 60, 50, 52] and the spin orbit effects of the pretzelosity function have been studied in both light-cone constituent quarks models [61, 62, 63, 64], while model predictions of azimuthal and transverse spin asymmetries have been predicted in [65, 50, 66].

The first model dependent extractions of the transversity distribution have been carried out [42] by combining SIDIS [28, 26, 67, 68] data with e^+e^- data [69] on the Collins function (see Figure 3). Within the uncertainties, the Soffer bound is respected. In addition, the extraction of the Siverts function [43, 44, 70, 71, 72] has been performed by combining SIDIS data from the HERMES [28] on the proton and COMPASS data [47] on the deuteron. The extracted Siverts functions from [43] are shown in Fig. 4. Complementing the data from the HERMES [28, 26], COMPASS [68], and BELLE [69] experiments, the recent release from the Jefferson Lab Hall A experiment E06-010 [73] on the neutron (with polarized ^3He) will facilitate a flavor decomposition of the transversity distribution function, h_1 [10, 74] and the Siverts distribution function f_{1T}^\perp [29]

in the overlapping kinematic regime. However a model-independent determination of these leading twist functions requires data in a wider kinematic range with high precision in *four dimensions* (Q^2, x, z, P_T).

In this paper, we discuss a newly approved experiment [75] with an 11-GeV electron beam, a high-pressure polarized ^3He target (as an effective polarized neutron target), and a solenoid detection system that will provide data with very high statistical and excellent systematic precision over a Q^2 range of 1 - 4 (GeV/c) 2 and a large range of x , z , and P_T values. The determination of the Collins, Sivers and pretzelosity asymmetries with high precision is very important to test theoretical predictions of TMDs and to improve our understanding of QCD.

4 The Experiment

4.1 Overview

This new experiment consists of a superconducting solenoid magnet, a detector system consisting of forward-angle detectors and large-angle detectors, and a high-pressure polarized ^3He target positioned upstream of the magnet. The polarized ^3He target is based on the technique of spin-exchange optical pumping of hybrid Rb-K alkali atoms. Such a target was used successfully in the recently completed SSA experiment [73] with a 6-GeV electron beam at JLab and an in-beam polarization of 60-65% was achieved. Design studies have been performed with both options of using the Babar and the CDF magnets. In this paper, we present the design with the option of the CDF magnet with a new yoke added. The upstream endcap plate will keep the magnetic field and its gradients under control in the target region. The field strength is simulated using the two-dimensional Poisson Superfish code. In this design, the absolute magnetic field strength in the target region is about a few Gauss with field gradients < 50 mG/cm. Correction coils around the target will further reduce field gradients to the desired level of ~ 30 mG/cm.

The layout of the experiment is shown in Fig. 5. The acceptance is divided into large-angle and forward-angle regions. The forward angle detectors cover the polar angle from 6.6 to 12 degrees with a momentum coverage from 0.9 to 7.0 GeV/c while the large angle side covers 14.5 to 22 degrees and 3.5 to 6.0 GeV/c. The total solid angle is about 57 msr for the forward-angle region and 231 msr for the large-angle region. Six layers of GEM detectors will be placed inside the coils as tracking detectors. A combination of an electromagnetic calorimeter, gas Čerenkov counters, a layer of Multi-gap Resistive Plate Chamber (MRPC) and a thin layer of scintillator will be used for particle identification in the forward-angle region. As only electrons will be identified in the large-angle region, a shashlyk-type [76, 77] electromagnetic calorimeter will be sufficient to provide the pion rejection.

4.2 The Detectors

4.2.1 Tracking and Resolutions

A total of six layers of GEM tracking detectors will be placed inside the magnet to determine the momentum, angle and vertex of the particles detected. Five layers of GEM detectors will be used for the forward-angle region. The first four layers will be sufficient for the large-angle region because the background level is expected to be much lower. The GEMs have worked for the COMPASS experiment [78, 79] in a flux of 30 kHz/mm 2 , which is much higher than the estimated rates in our configuration.

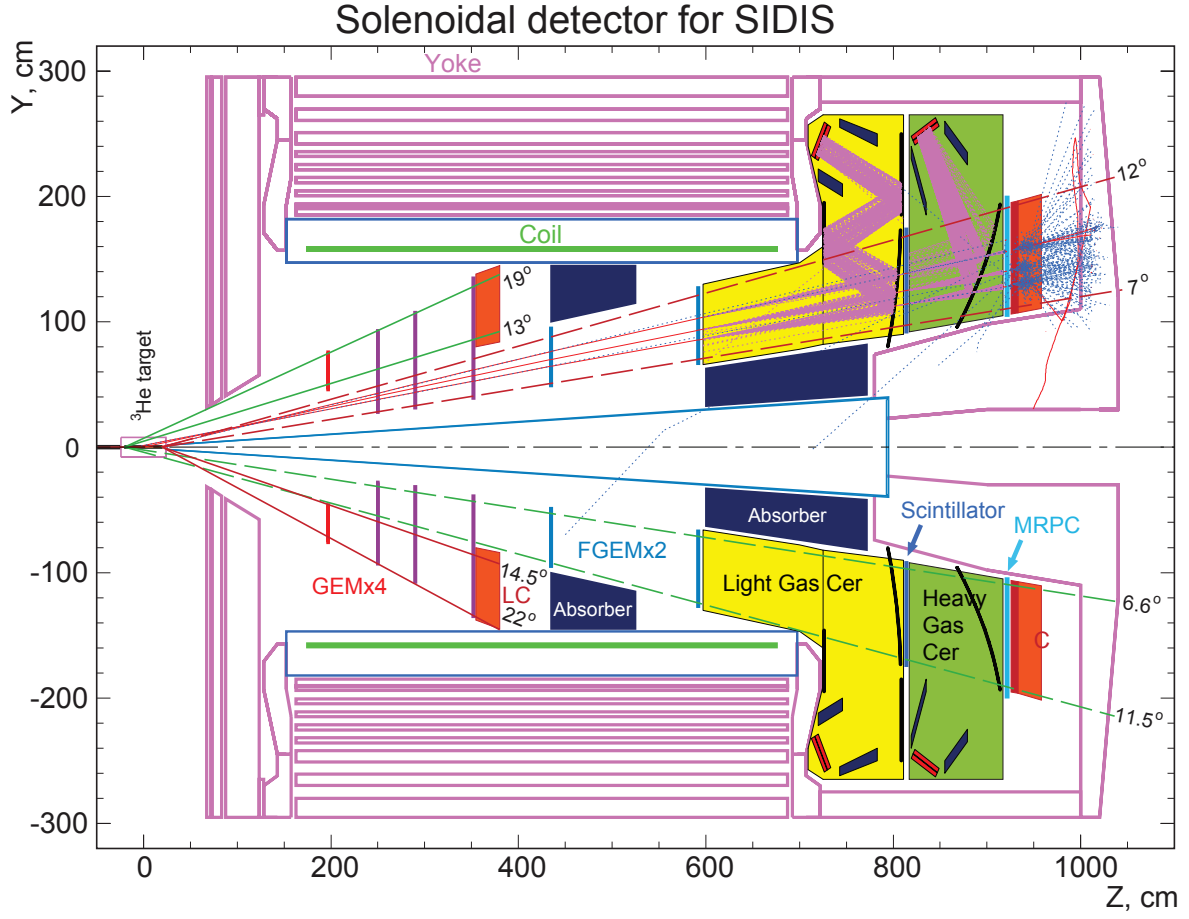


Figure 5: The experimental layout of the SoLID based on the option of using the CDF magnet. At forward angles, there are five layers of GEM detectors (The first three, in purple color, are shared with the large-angle detectors. The other two layers are in blue color.) inside the coils upstream of a 2.1-meter long light gas Čerenkov (yellow). One layer of scintillator (dark blue) will be placed after the light gas Čerenkov. A 1-meter long heavy gas Čerenkov (in green) is placed after the scintillator. One layer of Multi-gap Resistive Plate Chamber (MRPC) (light blue) is placed after the heavy gas Čerenkov. The electromagnetic calorimeters are shown in orange.

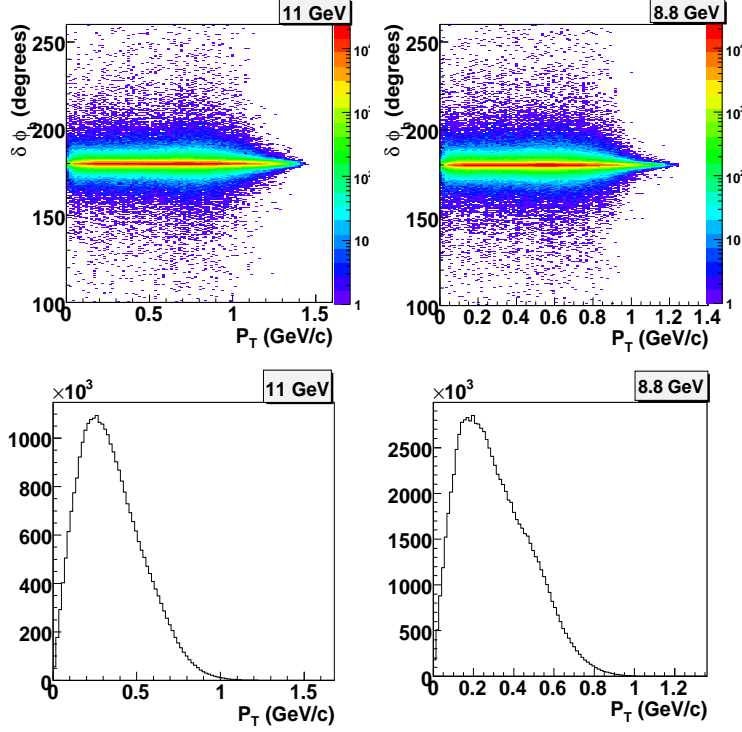


Figure 6: The $\delta\phi_h$ vs P_T are shown in top left (right) panel for 11 (8.8) GeV. The P_T coverage are shown in bottom left (right) panel for 11 (8.8) GeV.

To optimize the GEM configuration, a tracking MC simulation was performed, and a new tracking algorithm was developed based on the idea of progressive search[80]. The tracking MC study demonstrated that such a GEM configuration will work sufficiently well for the planned luminosity [75].

A simulation was performed to study the reconstruction resolutions with the CDF magnet. With the expected GEM resolution of $200\ \mu\text{m}$, the average momentum resolution, $\delta p/p$, is about 1.2%, and polar angle resolution is around 0.3 mrad while the azimuthal angular resolution is around 6 mrad. The average vertex resolution is about 0.8 cm over the entire momentum range. In addition to the polar and azimuthal angular resolution in the lab frame, the ϕ_h resolution was also studied and plotted versus the hadron transverse momentum P_T together with the P_T coverage as shown in Fig. 6. Here $\delta\phi_h$ is defined as the angle difference between the ϕ_h with and without the detector resolution effects. In Fig. 6, no clear resolution degradation is observed in $\delta\phi_h$.

4.2.2 Electron Identification

Two sets of electromagnetic calorimeters will be used to identify electrons in the forward and large-angle regions by measuring the energy deposition in the calorimeter through the electromagnetic shower. As discussed in more details in [81], a “shashlyk”-type calorimeter can be used inside the magnetic field and it is also radiation resistant. With a pre-shower/shower splitting, a

pion rejection factor of 200:1 can be achieved at $E > 3.5$ GeV and over 100:1 at $E > 1.0$ GeV.

To further improve the electron identification in the forward-angle region, two gas Čerenkov detectors will be used. Filled with CO₂ at 1 atmospheric pressure ($n=1.00045$), the light gas Čerenkov has a pion momentum threshold of 4.7 GeV/c. The 2-meter long setup is expected to produce about 17 photoelectrons for high energy electrons. As the overall background is estimated to be 40 MHz in such a detector, with 30 sectors and a 20-ns coincidence window, a 40:1 pion rejection can be achieved on-line, and the off-line pion rejection can be expected to be better than 80:1. The 80-cm long heavy gas Čerenkov detector filled with C₄F₁₀ at 1.5 atmospheric pressure ($n = 1.0021$) will provide additional suppression for pions with momentum up to 2.2 GeV/c. With 60 MHz background and about 25 photoelectrons for electrons in the detector, the pion rejection is expected to be better than 50:1.

The E06-010 (6 GeV transversity) [73] analysis shows that by requiring coincidence between pions and electrons in the DIS region, the pion contamination can be further reduced by about a factor of 5. Assuming a similar suppression factor in the kinematics of this experiment, the overall pion contamination in the electron sample can be controlled to be less than 0.2% for the coincident SIDIS events.

4.2.3 Pion Identification

For the forward-angle region, the identification of π^\pm with momentum between 0.9 to 7.0 GeV/c will be one of the major goals of the SIDIS experiment. The CO₂ gas Čerenkov and heavy gas Čerenkov detectors will separate pion from heavier hadrons with momentum range of 4.7 – 16 GeV/c and 2.2 – 7.6 GeV/c, respectively. The background rejections are about 80:1 and 50:1 from the two detectors.

In order to identify low-momentum pions, a multi-resistive plate chamber (MRPC) detector will be inserted after the two Čerenkov detectors and before the forward-angle calorimeter. A MRPC has been recently used in the STAR detector at RHIC and ALICE at LHC as their Time-Of-Flight detectors and its typical timing resolution is better than 80 ps. A MRPC does not need PMTs for readout so it can work inside a magnetic field. The simulated background rate on MRPC is shown to be less than 0.1 kHz/mm². Study [82] shows that the MRPC can work in an environment of background rate of 0.28 kHz/mm². The total path length is around 9 meters from the target and the flight time is calculated by comparing the TOF signal to the beam RF signal. With a TOF resolution of 100 ps, we can identify charged pions from charged kaons at a minimum rejection factor of 20:1 for a momentum range up to 2.5 GeV/c.

4.3 The Kinematics and Projections

The phase space coverage is obtained from a detailed Monte Carlo simulation based on GEANT3 which includes realistic spectrometer models as well as the target and detector geometry. The coverages in the (Q^2, x) , (W, x) , (W', x) , (p_T, x) , (z, x) and (p_T, z) are shown in Fig. 7 for a 11-GeV incident beam. The polar angles of electrons θ_e and pions θ_h have coverage from 6.6° to 22° and 6.6° to 12°, respectively. The momentum coverages for electrons and pions are from 1.0 GeV/c to 7.0 GeV/c. To ensure DIS kinematics, we will apply cuts for $Q^2 > 1$ (GeV/c)², $W > 2.3$ GeV and $W' > 1.6$ GeV (missing mass) to avoid the resonance region. The final kinematic coverage is $x = 0.05$ -0.65, $Q^2 = 1.0$ -8.0 (GeV/c)², which covers most of the region where the transversity distributions are significant. We choose to detect leading pions with $0.3 < z < 0.7$

to favor the current fragmentation region. The resulting transverse momentum of the hadron, P_T is between 0 and 1.6 GeV/c for an 11-GeV incident beam and between 0 and 1.2 GeV/c for an 8.8-GeV beam. Combining the 11 GeV and 8.8 GeV simulations results together, the total number of bins is about 1400. This will allow for a map of the SSAs in four dimensions (x , Q^2 , z and P_T).

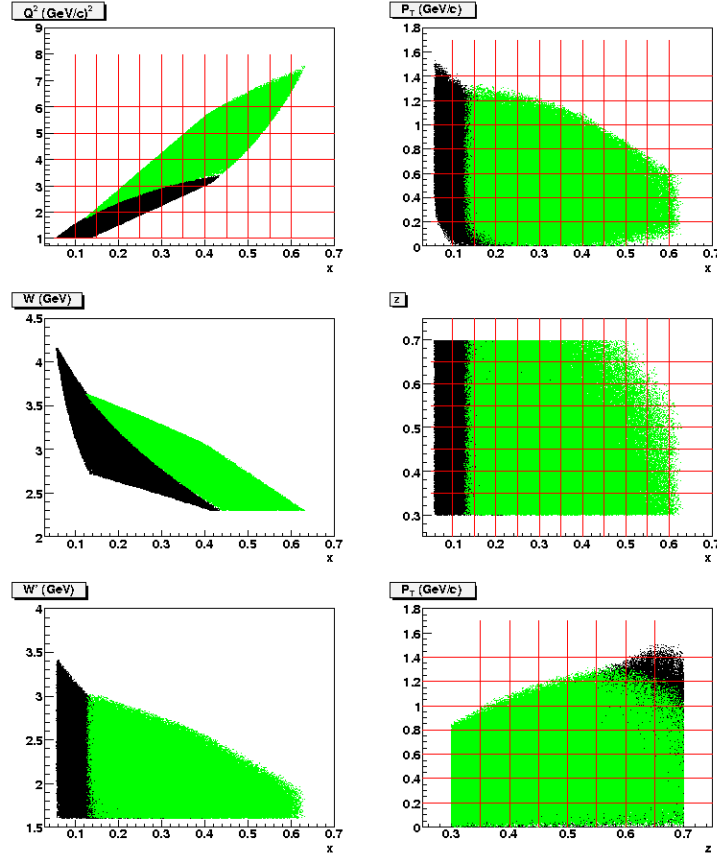


Figure 7: Kinematic coverage for the solenoid detector with a 11 GeV electron beam. The black points show the coverage for the forward-angle detectors and the green points show the coverage for the large-angle detectors.

Due to the nature of the large acceptance solenoid detector, we will have a complete 2π coverage for ϕ_S . The full 2π azimuthal angular coverage and a large ϕ_h azimuthal angular coverage are very important in disentangling different asymmetries (Collins, Sivers and Pretzelosity) to high precisions so that potential contributions from other azimuthal angular dependent terms due to higher-twist contributions ($\sin(\phi_S)$ and $\sin(2\phi_h - \phi_S)$) can be separated out.

The projected results for π^+ (π^-) Collins and pretzelosity asymmetries at one typical kinematic bin, $0.45 > z > 0.4$, $3 > Q^2 > 2$, are shown in Fig. 8 (Fig. 9) together with theoretical predictions of Collins asymmetries from Anselmino *et al.* [83], Vogelsang and Yuan [84] and predictions of Collins/pretzelosity asymmetries from Ma and collaborators [85, 62], and Pasquini [86, 64]. The projected E06-010 results are shown as black points. The x -axis is x_{bj} , and the y -axis on the left side is P_T , the transverse momentum of the hadron. The y -position

of the projections shows the average P_T value for the corresponding kinematic bin. The y -axis on the right side shows the scale of the asymmetry. The statistical uncertainties follow the scale on the right side of the y -axis as well as the theoretical calculations. The corresponding Sivers asymmetries for π^+ (π^-) are shown in Fig. 10 (Fig. 11).

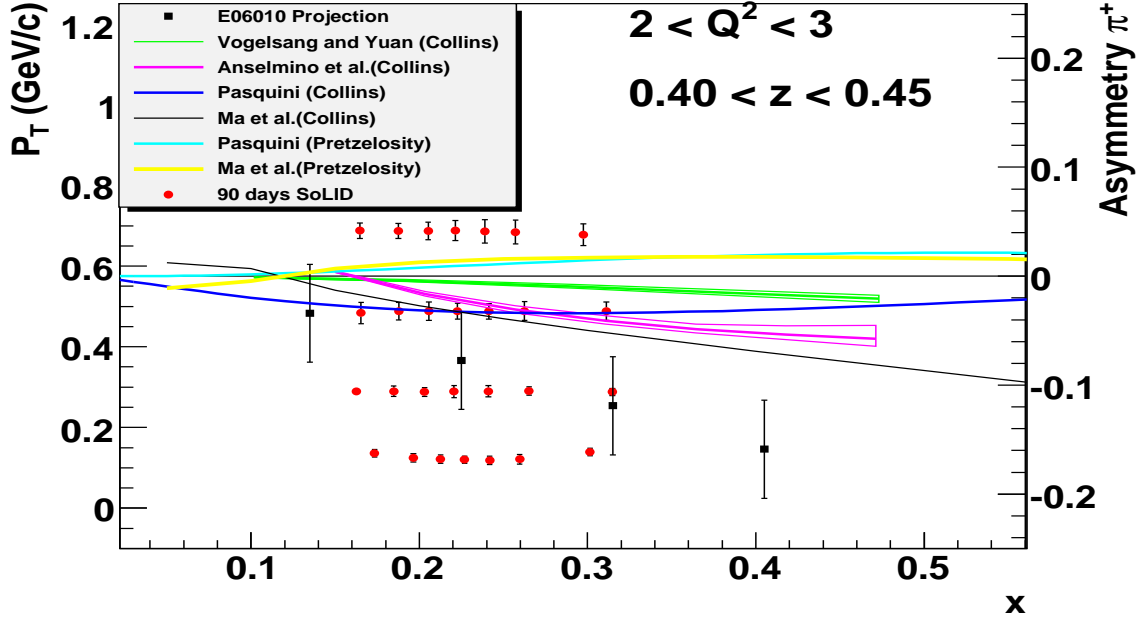


Figure 8: 12 GeV Projections with SoLID. π^+ Collins/pretzelosity asymmetries at $0.45 > z > 0.4$, $3 > Q^2 > 2$.

The complete projections for π^+ (π^-) Sivers asymmetries are shown in terms of 4-D (x , z , P_T and Q^2) kinematic bins in Fig. 12 (Fig. 13). Theoretical predictions of Sivers asymmetries from Anselmino *et al.* [83] and Vogelsang and Yuan [84] are shown in comparison ¹. We also include the current E06-010 projections in the first panel. The complete projections for π^+ (π^-) Collins/pretzelosity asymmetries in terms of 4-D (x , z , P_T and Q^2) are not presented here, but the statistics are comparable to those presented for the Sivers case.

By extending the study of SIDIS to a real 4-D manner (x , Q^2 , z and P_T), these new results will advance significantly our understanding of transverse spin physics. The Sivers distribution and the pretzelosity distribution functions, crucial to understand relativistic effects and the role of quark orbital angular momentum inside the nucleon, will also be mapped precisely in four dimensions in this new experiment. The large P_T region covered in this new experiment is important in testing various theoretical approaches. Further, a relatively large Q^2 region will allow for a study of the Q^2 evolution and higher-twist contributions ². Finally, extending the measurement of the transversity distribution to the large x region is essential to extract the tensor charge. A combined analysis between these proposed new neutron results and the future

¹The projections on Sivers asymmetry are shown separately from the projections of Collins and pretzelosity asymmetries, since the projection statistical uncertainties are different due to ϕ_h coverage.

²Higher twist effects can also be observed with contributions with $\sin(\phi_S)$ and $\sin(2\phi_h - \phi_S)$ angular modulation.

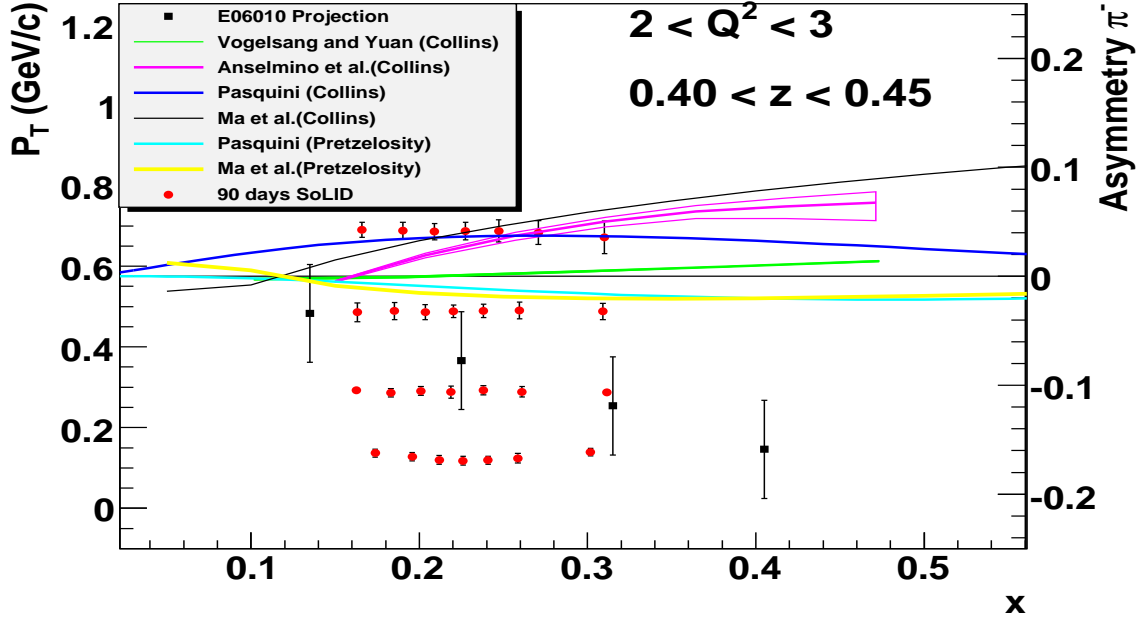


Figure 9: 12 GeV Projections with SoLID. π^- Collins/pretzelosity asymmetries at $0.45 > z > 0.4$, $3 > Q^2 > 2$.

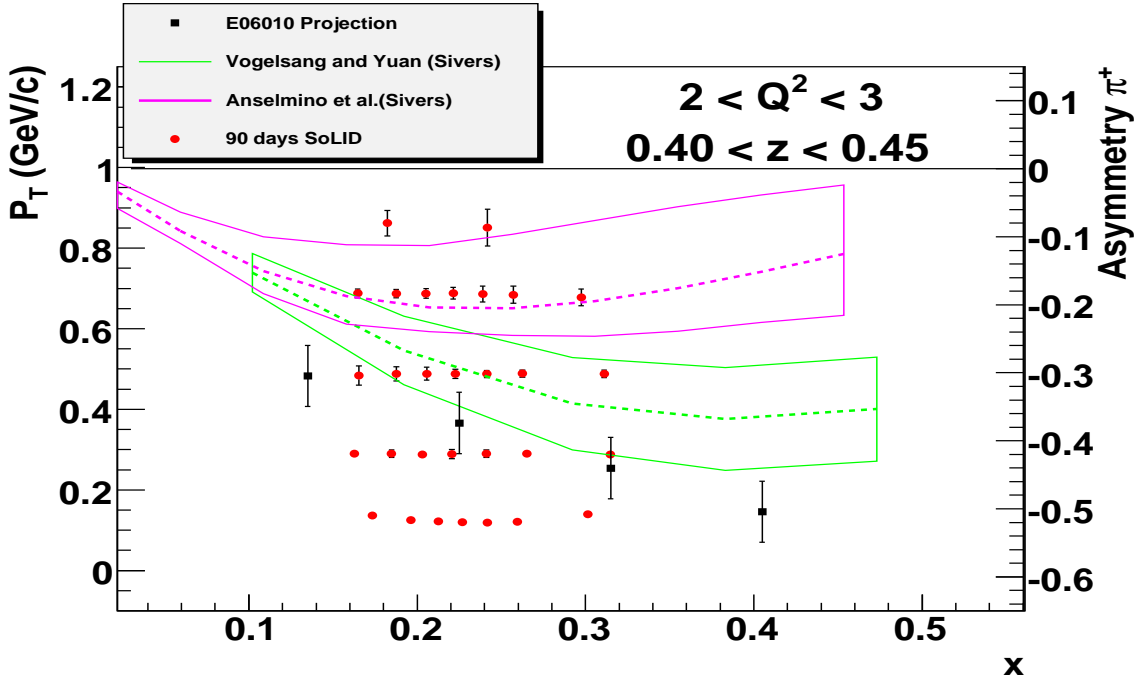


Figure 10: 12 GeV Projections with SoLID. π^+ Sivers asymmetries at $0.45 > z > 0.4$, $3 > Q^2 > 2$.

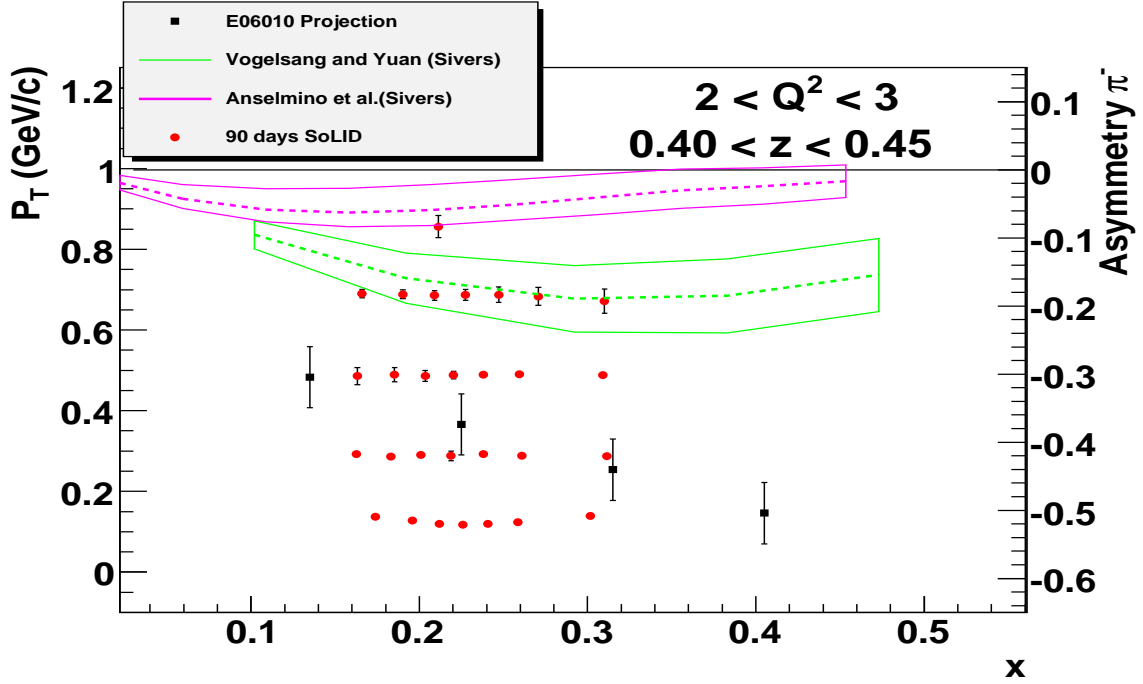


Figure 11: 12 GeV Projections with SoLID. π^- Sivers asymmetries at $0.45 > z > 0.4$, $3 > Q^2 > 2$.

proton results, will be carried out to extract the tensor charge of the u and d quark. The high statistics data from both the proton and the neutron will lead to a unprecedented precise determination of tensor charge. Such a precision will provide important tests of Lattice QCD predictions for the tensor charge.

5 Summary

Probing TMDs, in particular the transversity distribution, the least known leading-twist quark distribution function, which is non-zero upon integrating over the quark transverse momentum, is among the goals of several ongoing and future experiments. The experimental study of TMDs, which is now only at its inception, promises to have a very exciting future. Understanding the TMDs is certainly a complex task which demands major efforts in different laboratories in studying many different processes ranging over a wide kinematic region. This is a fast evolving field with growing interest worldwide. The new (SoLID) experiment discussed in this paper will provide SSA data with excellent statistical and systematic precisions in 4-D (x, z, P_T , and Q^2) over a large kinematic range. These data will significantly advance our understanding of TMDs and QCD. Measurements with SoLID, combined with the CLAS12 measurements [87, 88, 89, 90, 91] using polarized proton and deuteron targets will provide an unprecedented opportunity to obtain a three-dimensional map of the Collins and Sivers asymmetries in the kinematical region $0.1 < x < 0.5$, $0.3 < z < 0.7$ with $P_T < 1.5$ GeV, necessary to precisely determine the nucleon's partonic substructure. This new experiment will have a major impact on other related programs and particularly on the design of future facilities with the study of TMDs as one of their important

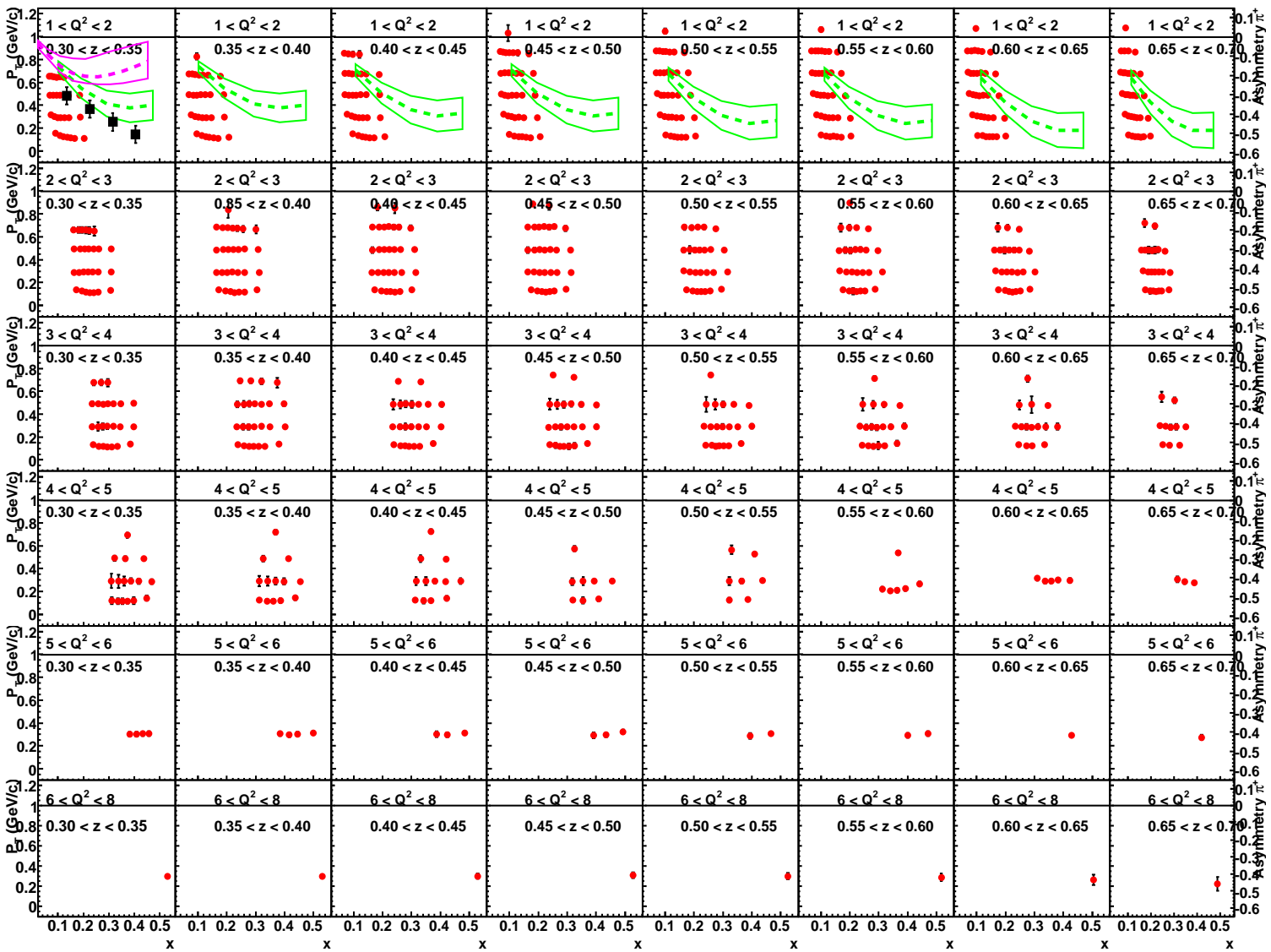


Figure 12: 12 GeV Projections with SOLID. π^+ Sivers asymmetries for all kinematic bin in terms of different z and Q^2 bin.

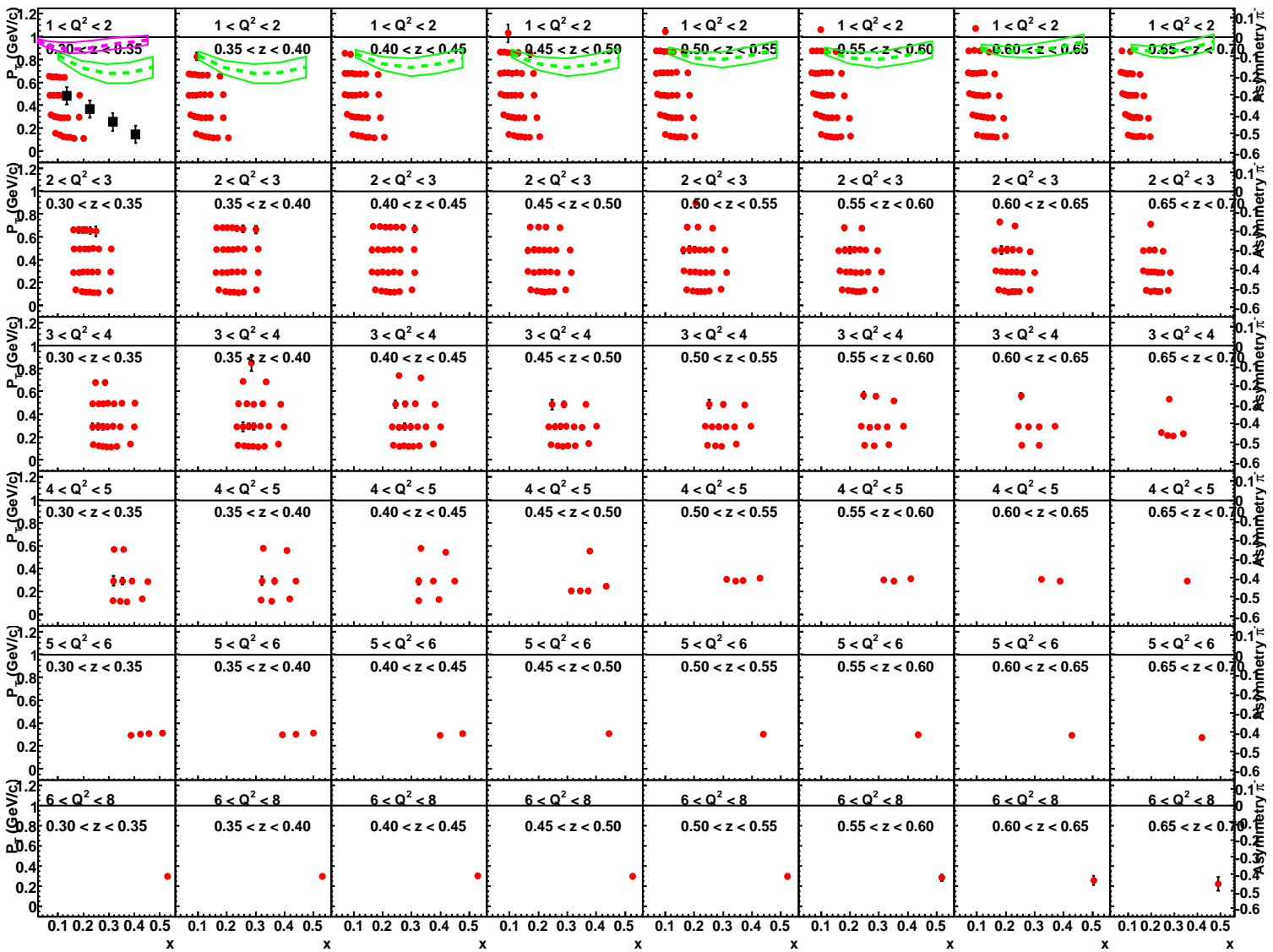


Figure 13: 12 GeV Projections with SOLID. π^- Sivers asymmetries for all kinematic bin in terms of different z and Q^2 bin.

physics goals, for example the electron ion collider (EIC), the FAIR project at GSI. It will also help to move theory forward in understanding and in modeling the quark TMDs significantly.

6 Acknowledgements

This work is supported in part by the U.S. Department of Energy under contracts, DE-AC05-84ER40150, modification No. M175, under which the Southeastern Universities Research Association operates the Thomas Jefferson National Accelerator Facility, DE-FG02-03ER41231 (H.G.), and DE-FG02-07ER41460 (L.G.).

References

- [1] European Muon, J. Ashman *et al.*, Phys. Lett. **B206**, 364 (1988).
- [2] B. W. Filippone and X.-D. Ji, Adv. Nucl. Phys. **26**, 1 (2001), hep-ph/0101224.
- [3] S. E. Kuhn, J. P. Chen, and E. Leader, Prog. Part. Nucl. Phys. **63**, 1 (2009), 0812.3535.
- [4] X. Artru and M. Mekhfi, Z. Phys. **C45**, 669 (1990).
- [5] P. J. Mulders and R. D. Tangerman, Nucl. Phys. **B461**, 197 (1996), hep-ph/9510301.
- [6] D. Boer and P. J. Mulders, Phys. Rev. **D57**, 5780 (1998), hep-ph/9711485.
- [7] X.-d. Ji, J.-P. Ma, and F. Yuan, Phys. Lett. **B597**, 299 (2004), hep-ph/0405085.
- [8] K. Hidaka, E. Monsay, and D. W. Sivers, Phys. Rev. **D19**, 1503 (1979).
- [9] J. P. Ralston and D. E. Soper, Nucl. Phys. **B152**, 109 (1979).
- [10] R. L. Jaffe and X.-D. Ji, Phys. Rev. Lett. **67**, 552 (1991).
- [11] V. Barone, Phys. Lett. **B409**, 499 (1997), hep-ph/9703343.
- [12] C. Bourrely, J. Soffer, and O. V. Teryaev, Phys. Lett. **B420**, 375 (1998), hep-ph/9710224.
- [13] J. Soffer, Phys. Rev. Lett. **74**, 1292 (1995), hep-ph/9409254.
- [14] W. Vogelsang, Phys. Rev. **D57**, 1886 (1998), hep-ph/9706511.
- [15] G. R. Goldstein, R. L. Jaffe, and X.-D. Ji, Phys. Rev. **D52**, 5006 (1995), hep-ph/9501297.
- [16] J. Ralston, private communications.
- [17] QCDSF, M. Gockeler *et al.*, Phys. Lett. **B627**, 113 (2005), hep-lat/0507001.
- [18] H.-X. He and X.-D. Ji, Phys. Rev. **D52**, 2960 (1995), hep-ph/9412235.
- [19] B. Q. Ma, I. Schmidt, and J. Soffer, Phys. Lett. **B441**, 461 (1998).
- [20] L. P. Gamberg and G. R. Goldstein, Phys. Rev. Lett. **87**, 242001 (2001), hep-ph/0107176.

- [21] I. C. Cloet, W. Bentz, and A. W. Thomas, Phys. Lett. **B659**, 214 (2008), 0708.3246.
- [22] M. Wakamatsu, Phys. Lett. **B653**, 398 (2007), 0705.2917.
- [23] B. Pasquini, M. Pincetti, and S. Boffi, Phys. Rev. **D72**, 094029 (2005), hep-ph/0510376.
- [24] J. C. Collins, Nucl. Phys. **B396**, 161 (1993), hep-ph/9208213.
- [25] HERMES, A. Airapetian *et al.*, (2010), hep-ex/1006.4221.
- [26] HERMES, A. Airapetian *et al.*, Phys. Rev. Lett. **103**, 152002 (2009), 0906.3918.
- [27] COMPASS, M. G. Alekseev *et al.*, (2010), 1005.5609.
- [28] HERMES, A. Airapetian *et al.*, Phys. Rev. Lett. **94**, 012002 (2005), hep-ex/0408013.
- [29] D. W. Sivers, Phys. Rev. **D41**, 83 (1990).
- [30] G. L. Kane, J. Pumplin, and W. Repko, Phys. Rev. Lett. **41**, 1689 (1978).
- [31] M. Anselmino, M. Boglione, and F. Murgia, Phys. Lett. **B362**, 164 (1995), hep-ph/9503290.
- [32] J. C. Collins, Phys. Lett. **B536**, 43 (2002), hep-ph/0204004.
- [33] A. V. Belitsky, X. Ji, and F. Yuan, Nucl. Phys. **B656**, 165 (2003), hep-ph/0208038.
- [34] D. Boer, P. J. Mulders, and F. Pijlman, Nucl. Phys. **B667**, 201 (2003), hep-ph/0303034.
- [35] S. J. Brodsky, D. S. Hwang, and I. Schmidt, Phys. Lett. **B530**, 99 (2002), hep-ph/0201296.
- [36] X.-d. Ji and F. Yuan, Phys. Lett. **B543**, 66 (2002), hep-ph/0206057.
- [37] L. P. Gamberg, G. R. Goldstein, and K. A. Oganessyan, Phys. Rev. **D67**, 071504 (2003), hep-ph/0301018.
- [38] M. Burkardt, Phys. Rev. **D69**, 057501 (2004), hep-ph/0311013.
- [39] M. Burkardt, Phys. Rev. **D72**, 094020 (2005), hep-ph/0505189.
- [40] S. J. Brodsky and S. Gardner, Phys. Lett. **B643**, 22 (2006), hep-ph/0608219.
- [41] M. Anselmino *et al.*, Nucl. Phys. Proc. Suppl. **191**, 98 (2009), 0812.4366.
- [42] M. Anselmino *et al.*, Phys. Rev. **D75**, 054032 (2007), hep-ph/0701006.
- [43] M. Anselmino *et al.*, Eur. Phys. J. **A39**, 89 (2009), 0805.2677.
- [44] M. Anselmino *et al.*, Phys. Rev. **D72**, 094007 (2005), hep-ph/0507181.
- [45] T.-c. Meng, J.-c. Pan, Q.-b. Xie, and W. Zhu, Phys. Rev. **D40**, 769 (1989).
- [46] M. Anselmino, M. Boglione, and F. Murgia, Phys. Rev. **D60**, 054027 (1999), hep-ph/9901442.
- [47] COMPASS, V. Y. Alexakhin *et al.*, Phys. Rev. Lett. **94**, 202002 (2005), hep-ex/0503002.

- [48] A. Bacchetta, A. Schaefer, and J.-J. Yang, Phys. Lett. **B578**, 109 (2004), hep-ph/0309246.
- [49] Z. Lu and B.-Q. Ma, Nucl. Phys. **A741**, 200 (2004), hep-ph/0406171.
- [50] L. P. Gamberg, G. R. Goldstein, and M. Schlegel, (2007), 0708.2580.
- [51] A. Bacchetta, F. Conti, and M. Radici, Phys. Rev. **D78**, 074010 (2008), 0807.0323.
- [52] B. Pasquini and F. Yuan, Phys. Rev. D **81**, 114013 (2010).
- [53] F. Yuan, Phys. Lett. **B575**, 45 (2003), hep-ph/0308157.
- [54] D. Amrath, A. Bacchetta, and A. Metz, Phys. Rev. **D71**, 114018 (2005), hep-ph/0504124.
- [55] A. Bacchetta, L. P. Gamberg, G. R. Goldstein, and A. Mukherjee, Phys. Lett. **B659**, 234 (2008), arXiv:0707.3372 [hep-ph].
- [56] A. Metz, Phys. Lett. **B549**, 139 (2002).
- [57] J. C. Collins and A. Metz, Phys. Rev. Lett. **93**, 252001 (2004), hep-ph/0408249.
- [58] L. P. Gamberg, A. Mukherjee, and P. J. Mulders, Phys. Rev. **D77**, 114026 (2008), 0803.2632.
- [59] G. R. Goldstein and L. Gamberg, (2002), Transversity and meson photoproduction Proceedings of ICHEP 2002; North Holland Amsterdam, p. 452 (2003), hep-ph/0209085, Published in Amsterdam ICHEP 452-454.
- [60] Z. Lu and B.-Q. Ma, Phys. Rev. **D70**, 094044 (2004), hep-ph/0411043.
- [61] H. Avakian *et al.*, Phys. Rev. D **78**, 114024 (2008).
- [62] J. She, J. Zhu, and B.-Q. Ma, Phys. Rev. D **79**, 054008 (2009).
- [63] B. Pasquini, S. Cazzaniga, and F. Yuan, Phys. Rev. D **78**, 034025 (2008).
- [64] S. Boffi, A. V. Efremov, B. Pasquini, and P. Schweitzer, Phys. Rev. **D79**, 094012 (2009), 0903.1271.
- [65] V. Barone, Z. Lu, and B.-Q. Ma, Phys. Lett. **B632**, 277 (2006), hep-ph/0512145.
- [66] V. Barone, A. Prokudin, and B.-Q. Ma, Phys. Rev. **D78**, 045022 (2008), 0804.3024.
- [67] COMPASS, E. S. Ageev *et al.*, Nucl. Phys. **B765**, 31 (2007), hep-ex/0610068.
- [68] COMPASS, M. Alekseev *et al.*, Phys. Lett. **B673**, 127 (2009), 0802.2160.
- [69] Belle, K. Abe *et al.*, Phys. Rev. Lett. **96**, 232002 (2006), hep-ex/0507063.
- [70] M. Anselmino *et al.*, (2005), hep-ph/0511017.
- [71] M. Anselmino *et al.*, Phys. Rev. **D71**, 074006 (2005), hep-ph/0501196.
- [72] J. C. Collins *et al.*, Phys. Rev. **D73**, 014021 (2006), hep-ph/0509076.

- [73] J. P. Chen *et al.*, Jlab E06-010.
- [74] V. Barone, A. Drago, and P. G. Ratcliffe, Phys. Rept. **359**, 1 (2002), hep-ph/0104283.
- [75] J. P. Chen *et al.*, Jlab E-10-006.
- [76] G. S. Atoian *et al.*, Nucl. Inst. Meth. **A531**, 467 (2004), 0310047.
- [77] G. S. Atoian *et al.*, Nucl. Inst. Meth. **A584**, 291 (2008), 0709.4514.
- [78] C. Altunbas *et al.*, Nucl. Inst. Meth. **A490**, 177 (2002).
- [79] P. Abbon *et al.*, Nucl. Inst. Meth. **A577**, 455 (2007).
- [80] R. Mankel, Rep. Prog. Phys. **67**, 553 (2004).
- [81] P. Souder *et al.*, Jlab E12-09-012.
- [82] Y. Wang *et al.*, Chinese Physics **C33**, 374 (2009).
- [83] M. Anselmino and A. Prokudin, private communications.
- [84] W. Vogelsang and F. Yuan, private communications.
- [85] H. Huang, J. She, and B.-Q. Ma, Phys. Rev. D **76**, 034004 (2007).
- [86] B. Pasquini, private communications.
- [87] CLAS(Collaboration), Jefferson Lab Letter-of-Intent LOI12-06-108 (2006).
- [88] H. Avakian *et al.*, Jefferson Lab Proposal E12-06-112 (2006).
- [89] H. Avakian *et al.*, Jefferson Lab Proposal E12-07-107 (2007).
- [90] H. Avakian *et al.*, Jefferson Lab Proposal E12-09-008 (2009).
- [91] H. Avakian *et al.*, Jefferson Lab Proposal E12-09-09 (2009).